XL CILAMCE
IBERO-LATIN AMERICAN CONGRESS ON COMPUTATIONAL METHODS IN ENGINEERING
NOVEMBER 11-14, 2019
Praiamar Natal Hotel & Convention Natal, RN-BRAZIL

# EVALUATION OF THE STRAIN ENERGY CAPACITY OF ARTIFICIAL TREES

**Paula de Oliveira Ribeiro**
*paula_ribeiro@usp.br*
*School of Engineering of São Carlos – EESC/USP*
*Av. Trabalhador Sãocarlense, 400, CEP: 13566-590, São Carlos, SP, Brazil*
**Gabriel Vilela**
**Marcelo Miranda Barros**
*gabriel.vilela@engenharia.ufjf.br*
*marcelo.barros@ufjf.edu.br*
*Federal University of Juiz de Fora*
*Rua José Lourenço Kelmer, s/n, CEP:36036-900, Juiz de Fora, MG, Brazil*

**Abstract.** Nowadays much effort in science and technology is related to renewable energy, once the actual society is based on available energy and the demand is increasing. One of the actual research areas in harvesting energy is based on vibration using piezoelectric materials. Natural trees are known to be very flexible and resilient. Trees are able to absorb relatively high quantities of energy from the wind due to their flexibilities as well as the high drag force induced by the leafs. Piezoelectric energy harvesters must contain flexible elements in order to induce vibration within its elements, since the strain rate is necessary to induce electrical current within these devices. Artificial trees with a given number of generations may be built by fractal geometry, or iterated function systems. In this paper we propose a 2D model for the trees extended to 3D by unitary depth. Thus, the geometrical properties of each branch are the length and the width. The trees are self-similar, i.e. the quantity of children for each father branch is constant for all branching, as well as the length and width ratios, given by the parameters $b$, $\lambda$ and $w$ respectively. Let $n$ be the number of generations, or iterations, and $\lambda_0$ and $w_0$ the length and width of the trunk. Therefore an infinity of trees may be generated through this set of six parameters. In this paper we present analytical expressions for the strain energy in tree structures generated by fractal geometry. Some numerical experiments are performed in order to both confirm the analytical propositions and evaluate the strain energy for some particular structures.

**Keywords:** Renewable energy, Piezoelectric devices, Fractal trees

# 1 Introduction

With increasing demand for energy and the need to develop green and renewable energy alternatives, researchers have been struggling to develop effective energy generation systems. One of the current research areas is energy harvesting [1, 2]. Energy harvesting consists in converting environmental energy into electrical energy.

Piezoelectric generators employ active materials that induce movement of electrical charge when mechanically requested, i.e., convert mechanical energy into electrical energy [1]. By means of the strain, there is an electric potential difference. Commonly used piezoelectric materials are films, for example, PVDF (PolyVinylidene Fluoride), or piezoelectric ceramic, e.g. PZT (Lead Zirconate Titanate) [2]. Castagnetti and Radi [3] mentioned the power of self-sustaining electronic devices and remote sensors as a direct application of energy harvesting for the exploration of the piezoelectric effect, which would guarantee continuous operation over a long period of time.

Some recent researches study the application of structures described by fractal geometry in energy harvesting [3, 4, 5]. Fractal geometry was proposed by Mandelbrot [6], making possible the description of irregular structures that were not described by Euclidean geometry. According to Nussenzveig [7], fractals are sets whose shape is extremely irregular or fragmented and which have essentially the same structure at all scales.

Researchers have proposed antennas generated by fractal geometry in order to harvest energy by radiofrequency, since the fractal geometries have the capacity to operate in different frequency bands at the same time with smaller physical sizes [8]. Çelik and Kurt [8] designed and simulated a multi-band fractal antenna, Fig. 1 (a), used in radiofrequency energy capture systems, the analyses showed the potential of the antenna to supply electronic components, such as wireless sensor networks. Puente et al. [9] showed that an antenna with the shape of a tree presents a multiband behavior with a dense band distribution. Bakytbekov et al. [10] proposed a fully printed 3D cube-shaped multiband fractal rectenna for ambient radio frequency energy harvesting, Fig. 1 (b). Palandoken and Gocen [11] proposed a modified Hilbert fractal resonator, Fig. 1 (c), according to the authors the numerical and experimental results point out the potential of the design to be used in low power electronic devices.

(a) (b) (c)

Figure 1. Fractal geometries applied in energy harvesting (a) 1st, 2nd and 3rd iteration of fractal geometry [8] (b) 3D cube antenna [10] (c) Modified Hilbert fractal resonator [11]

In the present paper, we derived expressions to the strain energy in tree-like fractal structures in order to evaluate the possibility for using such patterns to harvest energy from vibration. Trees are able to absorb relatively high amounts of wind energy due to their flexibilities as well as to the high drag force induced by the leaves.

In this work, we perform analytical and numerical models about the mechanical behavior of self-similar trees, i.e., evolved in terms of pre-defined constant proportions between parent and child branches [12]. Two models with different external loads were considered: concentrated moment or horizontal force at the free ends. The first is the reference and the second is to represent the wind in a static way.

# 2 Methodology

The aim of this paper is to find general expressions for the strain energy within trees as function of the geometric parameters and to validate the expressions through numerical analysis using a commercial software for particular trees. For this purpose, two models of trees with different external loads were studied: moments or horizontal forces applied at the extremities.

## 2.1 Geometric model

The geometry of self-similar trees is defined by three parameters that relate quantity, length and width (for a 2D model) between parent and child branches in all orders of the tree and are represented, respectively, by $b$, $\lambda$, $w$. Also, $k = 0,1,...,n-1$ is the counter for the orders, $n$ is the evolutionary parameter which indicates the number of orders, $N_k$ is the number of elements in order $k$, $\lambda_k$ is the length of the elements and $w_k$ is the width of the elements in order $k$. Thus, the geometric parameters are defined as follows:

$$b = \frac{N_{k+1}}{N_k}, \tag{1}$$

$$\lambda = \frac{\lambda_k}{\lambda_{k+1}}, \tag{2}$$

$$w = \frac{w_k}{w_{k+1}}. \tag{3}$$

The complete generation of a tree is made by the parameters $b$, $\lambda$ and $w$, by the evolutionary parameter $n$ and by the initial trunk $\lambda_0$, $w_0$. Figure 2 shows an example of self-similar tree with the same values for $w$ and $\lambda$, exhibiting geometric similarity.

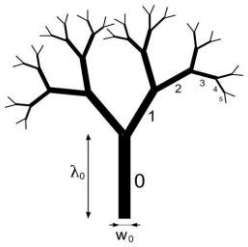


Figure 2. Example of self-similar tree with parameters $b = 2$, $\lambda = 1.5$, $w = 1.5$ and $n = 6$ [13]

## 2.2 Mechanical model

The proposed self-similar geometric model has the same relation between parent and child elements throughout the tree, i.e., $b$, $\lambda$ and $w$ are constants. Each set of parameters generates trees with different mechanical behavior. The proposed models consist of self-similar trees where the elements are considered as bars with linear elastic behavior. The main trunk is considered clamped to the ground while the extremities are free and submitted to external loads. Two sets of external loads where considered, namely models 0 and 1.

In model 0 all extremities receive action of concentrated moments. As a consequence, the bars transmit this moment evenly along each element and a parent branch receives the moments coming from their child branches. As consequence the inclination of the bars when the action is given by external moments does not influence the bending moment along the bars. Thus, the expression for the energy becomes relatively simple for this model.

In model 1 all the extremities receive the action of horizontal forces. The bending effect generated within the bars depends on the distance of the forces to the sections in the bars and therefore, within each bar the bending moment is not constantly distributed and the branching angles influences the bending moments within the bars. In order to make the deduction of expressions possible the bars will

be considered with null angles, i.e., vertical, because in this case the bending moments are maximized and thus the worst case will be studied. In this model the vertical bars are considered flexible and the horizontal bars are rigid, so that the horizontal bars do not influence the mechanical analysis of the structure. The model 1 with horizontal forces can be used to represent the wind action statically. Figure 3 shows the models 0 and 1.

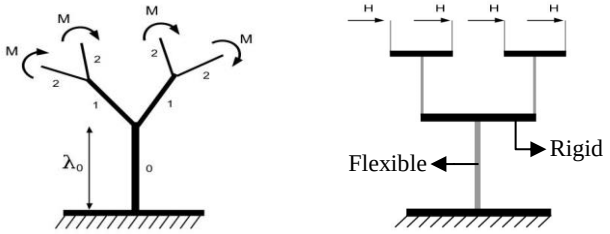


(a) (b)

Figure 3. Representation of models (a) model 0 (b) model 1 [13]

## 3 Analytical results

### 3.1 Expressions for bending moment and strain energy

The analytical study consists in the deduction of expressions that describe the bending moment and strain energy along the tree. The aim of this study is to evaluate the influence of the parameters $b$, $\lambda$, $w$ and n on the mechanical properties.

The bending moment is the cause of the bending that occurs in a bar when subjected to forces. The relative momentum is defined by the ratio between the maximum bending moments in consecutive orders, that is, $m = M_k^{\max} / M_{k+1}^{\max}$.

The strain energy is the increase of energy within a member when undergoing an elastic deformation. In a bar of length $L$, Young modulus $E$ and moment of inertia $I$ subject to a bending moment $M(s)$, the elastic energy is obtained by Eq. (4).

$$W = \frac{1}{2}\int_0^L \frac{M(s)^2}{EI}\,ds \tag{4}$$

In Table 1 are the expressions of bending moment and strain energy developed for models 0 and 1, in absolute and relative value.

Table 1. Expressions of bending moment and strain energy

| Model | Property | Absolute value | Relative value |
|---|---|---|---|
| Model 0 | Bending moment | $M_k = Mb^{n-k-1}$ | $m = b$ |
| | Strain energy | $W_k = 6\dfrac{b^k \lambda_0 \lambda^{-k} (Mb^{n-k-1})^2}{E w_0^{\,3} w^{-3k}}$ | $W = \dfrac{b\lambda}{w^3}$ |
| Model 1 | Bending moment | $M_k = Hb^{n-k-1}\sum_{i=k}^{n-1}\lambda_i$ | $m = bh_k(\lambda)$ |
| | Strain energy | $W_{n-K-1} = \dfrac{H^2 b^{2K} N_{n-K-1}\lambda_{n-K-1}}{2EI_{n-k-1}\lambda^{2K}} g_k(\lambda)$<br>$W_{n-1} = \dfrac{N_{n-1}H^2\lambda_{n-1}^3}{6EI_{n-1}}, K = 0$ | $W = \dfrac{b\lambda}{I}\bar{g}_k(\lambda)$ |

$h_k(\lambda) = \dfrac{1+\lambda+\lambda^2+\ldots+\lambda^{n-k-1}}{1+\lambda+\lambda^2+\ldots+\lambda^{n-k-2}}$; $g_K(\lambda) = \sum_{i=1}^{K}(i\lambda^{i-1}+(K-i+1)\lambda^{i+K-1}) + \dfrac{\lambda^{2K}}{3}$; $\bar{g}_K(\lambda) = \dfrac{\sum_{i=1}^{K}(i\lambda^{i-1}+(K-i+1)\lambda^{i+K-1}) + \frac{\lambda^{2K}}{3}}{\sum_{i=1}^{K-1}(i\lambda^{i-1}+(K-i)\lambda^{i+K-2}) + \frac{\lambda^{2(K-1)}}{3}}$, where $K = n-k-1$.

Table 2 shows the influence of the parameters $b$, $\lambda$ and $w$ in the region within the tree of maximum values of properties.

Table 2. Correlation between the geometric parameters and the mechanical behavior

| Model | Property | Condition | Mechanical behavior |
|---|---|---|---|
| Model 0 | Bending moment | - | Maximum at the trunk |
| | Strain energy | $w < \sqrt[3]{b\lambda}$ | Maximum at the trunk |
| | | $w > \sqrt[3]{b\lambda}$ | Maximum at extremities |
| | | $w = \sqrt[3]{b\lambda}$ | Constant |
| Model 1 | Bending moment | - | Maximum at the trunk |
| | Strain energy | $w < \sqrt[3]{b\lambda^3}$ | Maximum at the trunk |
| | | $w > \sqrt[3]{b(\lambda^3 + 3\lambda^2 + 3\lambda)}$ | Maximum at extremities |

### 3.2 Efficiency in storing energy for model 0

In this item will be presented the study about the efficiency in the elastic energy abortion of a branched structure in comparison with a cylinder of same volume. In the evaluation of model 0, it was considered a concentrated moment $M$ in the cylinder and at the free ends of the tree was considered $\alpha M$, with α equals to $1/b^{n-1}$ and 1, representing, respectively, the situation in which the load is divided between all ends and the situation where all extremities receive the full load. Figure 4 shows an example of a tree and a unique trunk with same volume of the tree to be compared.

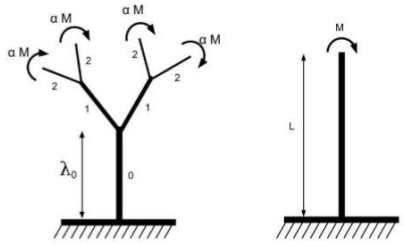


Figure 4. Branched structure and a sole trunk with concentrated moment at extremities [13]

The length $L$ of the sole trunk was chosen such that the total volume of the sole trunk was equal to the volume of the branched structure. Equation (5) presents the expression of $L$ by considering the width of the sole trunk equal to $w_0$ and using the geometric parameters presented in Eq. (1), (2) and (3).

$$L = \lambda_0 \sum_{k=0}^{n-1} \left( \frac{b}{w\lambda} \right)^k \tag{5}$$

Based on the expressions presented in Table 1, the total energy within a tree of model 0 may be obtained by Eq. (8).

$$W_{TOTAL} = W_0 + W_1 + W_2 + ... + W_{n-1} \tag{6}$$

$$W_{TOTAL} = W_0 \sum_{k=0}^{n-1} (W^{-1})^k \quad \therefore \quad W_{TOTAL} = W_0 \frac{(W^{-1})^n - 1}{W^{-1} - 1} \tag{7}$$

$$W_{TOTAL} = \left( \frac{12\lambda_0 M^2 b^{2n-2}}{2E{w_0}^3} \right) \left( \frac{\left( \frac{w^3}{b\lambda} \right)^n - 1}{\left( \frac{w^3}{b\lambda} \right) - 1} \right) \tag{8}$$

The total energy of the cylinder may be obtained by Eq. (9).

$$\bar{W} = 6\frac{M^2}{Ew_0^3}\lambda_0 \sum_{k=0}^{n-1}\left(\frac{b}{w\lambda}\right)^k \tag{9}$$

The efficiency in absorbing energy is defined as the ratio of the total energy stored within the tree structure to the total energy stored in the sole trunk where both have the same volume:

$$e = \frac{W_{TOTAL}}{\bar{W}}. \tag{10}$$

Substituting Eq. (8) and (9) into Eq. (10) it is obtained the efficiency in terms of the parameters of the geometry as:

$$e = \left(\frac{\left(\frac{w^3}{b\lambda}\right)^n - 1}{\left(\frac{w^3}{b\lambda}\right) - 1}\right)\left(\frac{\alpha^2 b^{2n-2}}{\sum_{k=0}^{n-1}\left(\frac{b}{\lambda w}\right)^k}\right). \tag{11}$$

The graphs of Fig. 5 show the efficiency for the two of $\alpha$. It is observed that the efficiency increases with increasing $b$ for $\alpha = 1$ (Fig. 5.a) and the efficiency decreases with increasing $b$ for $\alpha = 1/b^{n-1}$ (Fig. 5.b). The graphs in Fig. 5.c and Fig. 5.d show that efficiency increases with the addition of *n*.

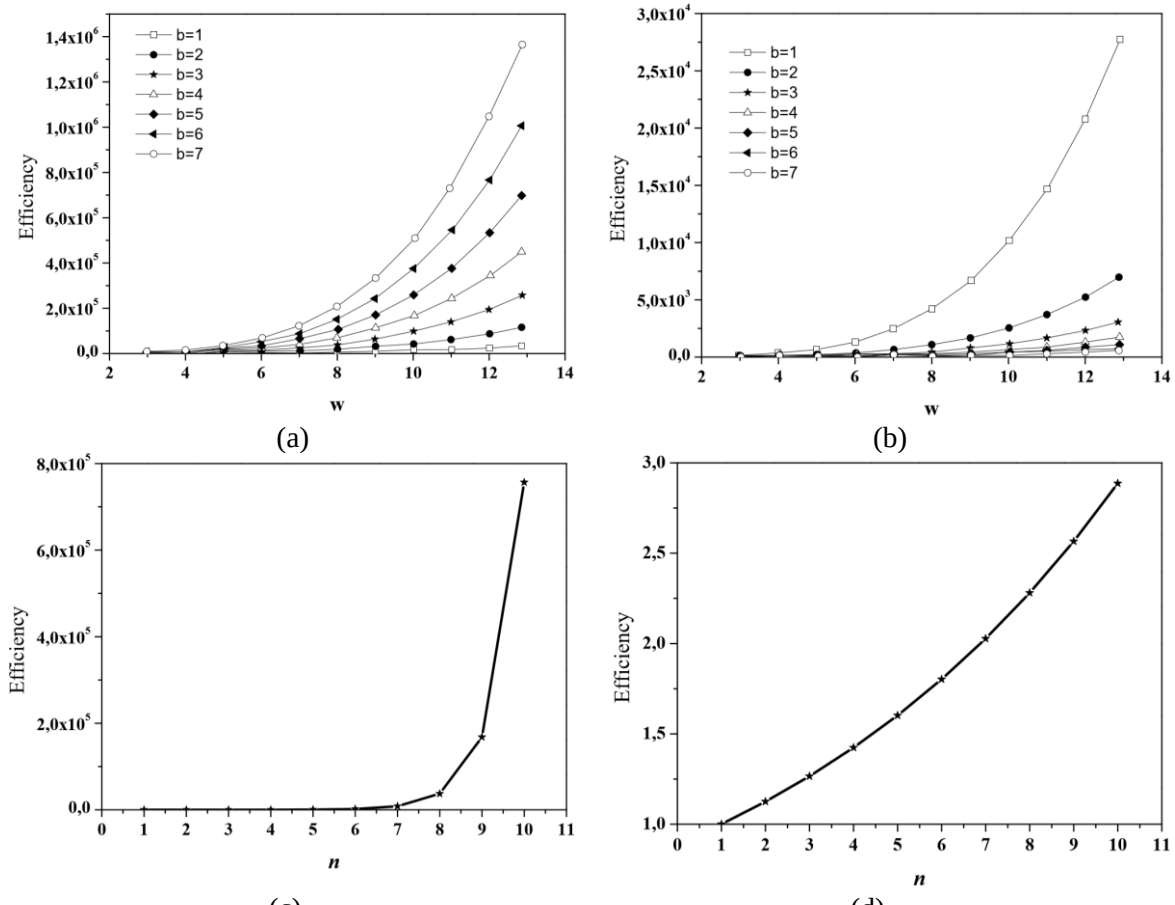


Figure 5: Efficiency of the branched structure for model 0 (a) $n = 3, \alpha = 1$ (b) $n = 3,\ \alpha = 1/b^{n-1}$ (c) $b = 2, \lambda = w = 1.5,\ \alpha = 1$ (d) $b = 2, \lambda = w = 1.5,\ \alpha = 1/b^{n-1}$

### 3.3 Efficiency in storing energy for model 1

The efficiency of model 1 with relation to the sole trunk was also analyzed. Figure 6 shows the models evaluated.

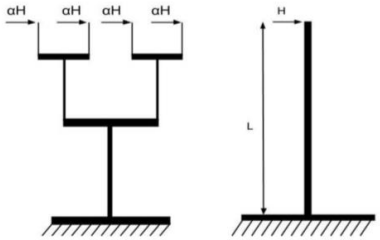


Figure 6. Branched structure and constant section cylinder with load concentrated at the end [13]

The total energy of model 1 is calculated by the sum of the energy of each order, Eq. (12). Based on the expressions presented in Table 1, the total energy of model 1 is calculated by Eq. (14).

$$W_{TOTAL} = W_0 + W_1 + W_2 + ... + W_{n-1} \tag{12}$$

$$W_{TOTAL} = W_{n-1} + \sum_{K=1}^{n-1} W_{n-K-1} \tag{13}$$

$$\sum_{K=1}^{n-1} W_{n-K-1} = \sum_{K=1}^{n-1} 6\left( \frac{\alpha^2 H^2 b^{2K} b^{n-K-1}}{E\lambda^{2K}} \cdot \left( \frac{\lambda_0}{w_0} \right)^3 \cdot \left( \frac{w}{\lambda} \right)^{3(n-K-1)} \cdot \left[ \sum_{i=1}^{K} \left( i\lambda^{i-1} + (K-i+1)\lambda^{i+K-1} \right) + \frac{\lambda^{2K}}{3} \right] \right) \tag{14}$$

For model 1, the bending moment along the cylinder is given by $M(s) = H \cdot s$. Substituting the value of the moment in Eq. (4), the total energy of the sole trunk is deduced.

$$\bar{W} = 2\frac{H^2}{Ew_0{}^3} \left( \lambda_0 \sum_{k=0}^{n-1} \left( \frac{b}{w\lambda} \right)^k \right)^3 \tag{15}$$

The efficiency is defined by the ratio between the total energy of the branched structure and a cylinder of the same volume, obtained as:

$$e = \frac{2\frac{b^{n-1}\alpha^2 H^2 \lambda_0{}^3 \lambda^{-3(n-1)}}{Ew_0{}^3 w^{-3(n-1)}} + \sum_{K=1}^{n-1} 6 \cdot \left( \frac{\alpha^2 H^2 b^{2K} b^{n-K-1}}{E\lambda^{2K}} \cdot \left( \frac{\lambda_0}{w_0} \right)^3 \cdot \left( \frac{w}{\lambda} \right)^{3(n-K-1)} \cdot \left[ \sum_{i=1}^{K} \left( i\lambda^{i-1} + (K-i+1)\lambda^{i+K-1} \right) + \frac{\lambda^{2K}}{3} \right] \right)}{2\frac{H^2}{Ew_0{}^3} \left( \lambda_0 \sum_{k=0}^{n-1} \left( \frac{b}{w\lambda} \right)^k \right)^3}. \tag{16}$$

Figure 7 show the efficiency for the two values of $\alpha$. It is observed that the efficiency increases with increasing $b$ for $\alpha = 1$ (Fig. 7.a) and the efficiency decreases with increasing $b$ for $\alpha = 1/b^{n-1}$ (Fig. 7.b). The graphs in Fig. 7.c shows that efficiency increases with *n* for $\alpha = 1$ and Fig. 7.d shows that efficiency decreases with *n* for $\alpha = 1/b^{n-1}$.

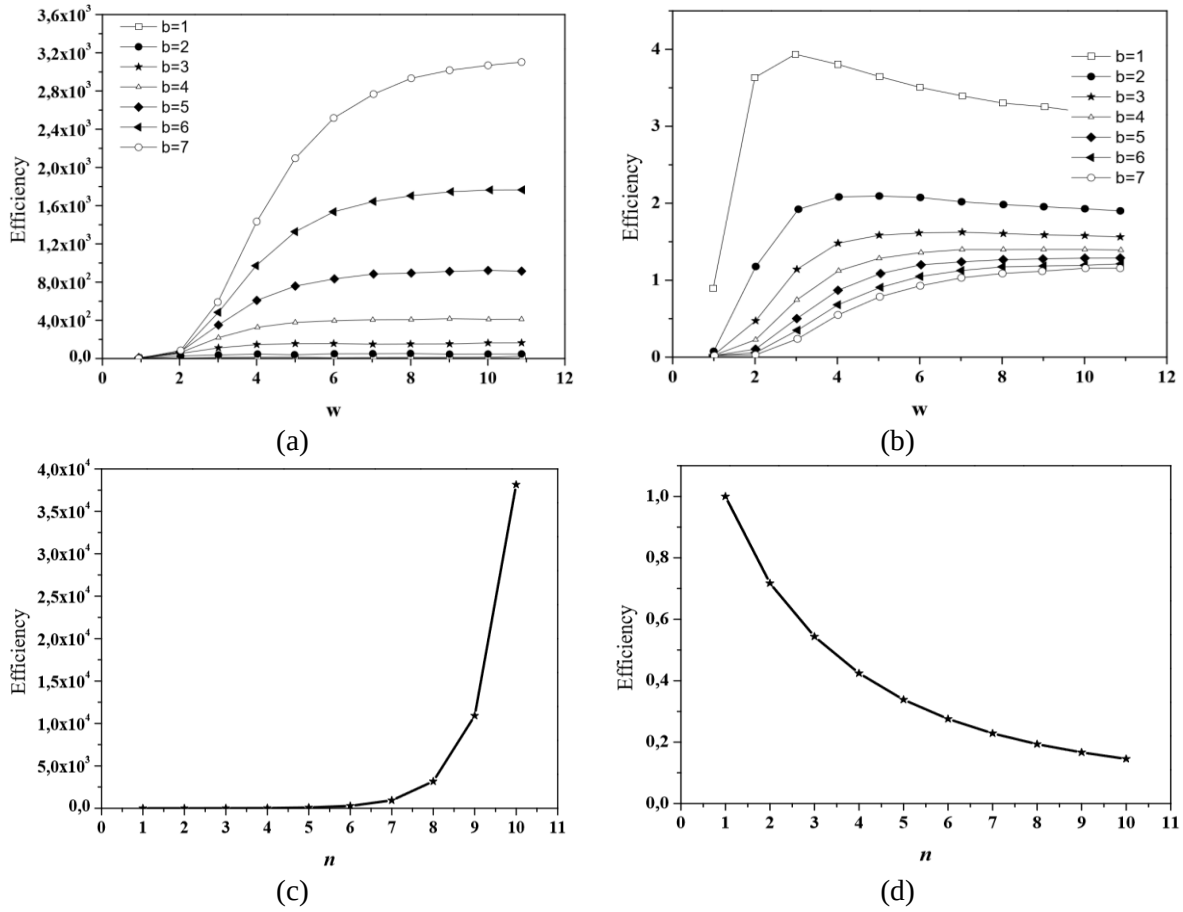


Figure 7: Efficiency of the branched structure in relation to the cylinder - Model 1 (a) $n=3, \alpha=1$ (b) $n=3,\ \alpha=1/b^{n-1}$ (c) $b=2, \lambda=w=1.5,\ \alpha=1$ (d) $b=2, \lambda=w=1.5,\ \alpha=1/b^{n-1}$

## 4 Computational simulation

In this section numerical simulations were performed in order to validate, for particular cases, the expressions presented in Table 1. In doing so we used the software Ansys Student Workbench. The numerical model was simulated with the parameters presented in Table 3.

Table 3. Parameters adopted in the numerical model

| Geometrical parameter | Model 0 | Model 1 |
|---|---|---|
| $\lambda_0\ (m)$ | 10 | 10 |
| $w_0\ (m)$ | 1 | 1 |
| $b$ | 2 | 2 |
| $\lambda$ | 1.5 | 1.5 |
| $w$ | 1.5 | 1.5 |
| $n$ | 4 | 4 |
| $M\ (N.m)$ | 1 | - |
| $H\ (N)$ | - | 1 |
| $E\ (N/m^2)$ | $1.3\times10^{10}$ | $1.3\times10^{10}$ |

The numerical model was elaborated with a mesh composed of 648 elements and 5586 nodes. The element type used was SOLID186. This element is a 3D solid element with 20 nodes per element and three degrees of freedom per node and exhibits quadratic displacement behavior. Figure 8 shows simulated models.

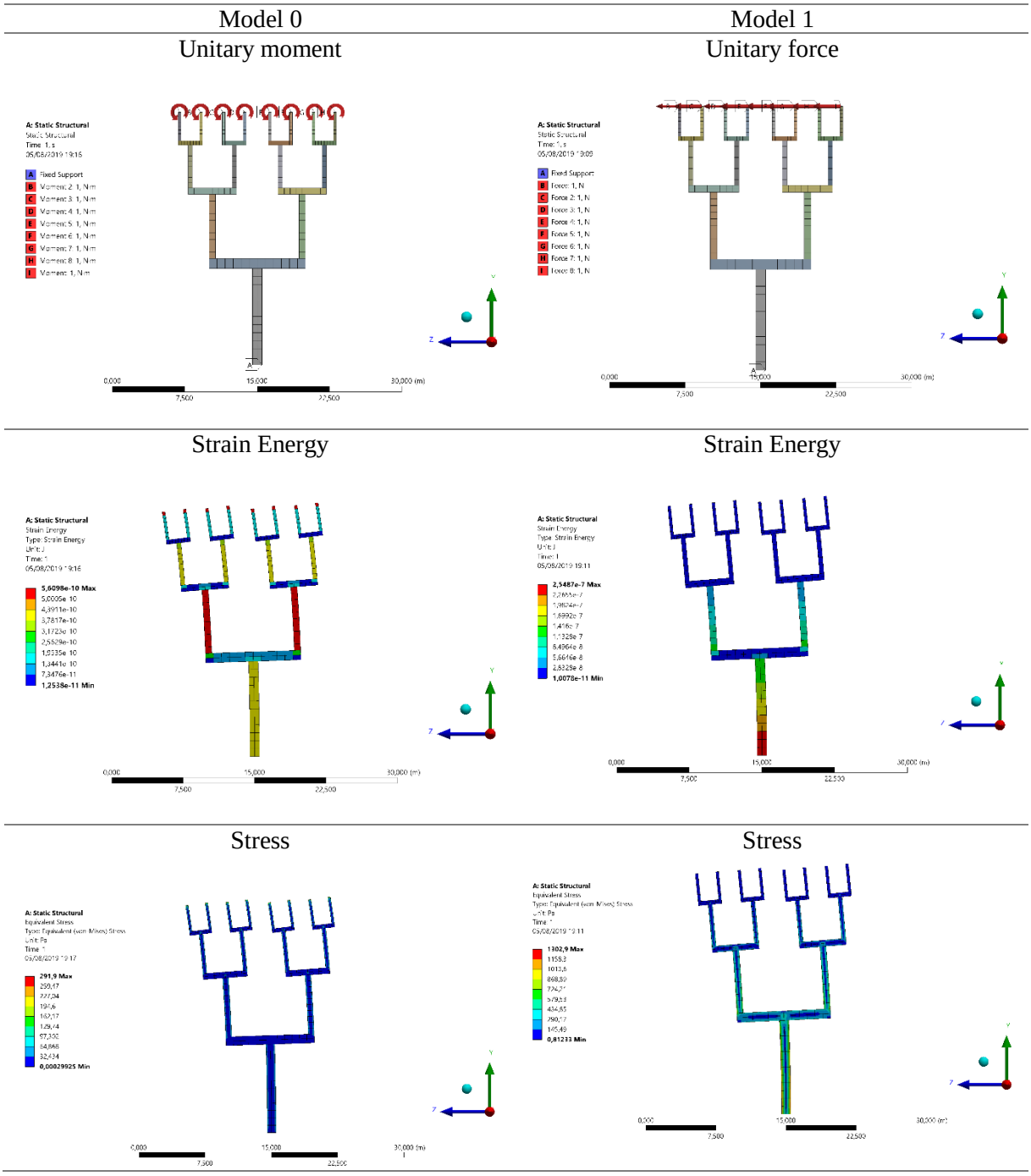


Figure 8: Simulation of models in ANSYS

The results obtained by the numerical model were compared with the results obtained by the expressions presented in Table 1. Tables 4 and 5 show that the results were very close.

Table 4. Comparison between numerical and analytical results (Model 0)

| Order | Model 0 | | | | | |
|---|---|---|---|---|---|---|
| | Maximum moment (N.m) | | | Strain energy (J) | | |
| | Analytical | Numerical | Error (%) | Analytical | Numerical | Error (%) |
| 0 (trunk) | 8.000 | 8.000 | 0 | 2.954E-07 | 2.936E-07 | 0.597 |
| 1 | 4.000 | 4.0022 | 0.055 | 3.323E-07 | 3.306E-07 | 0.502 |
| 2 | 2.000 | 2.0091 | 0.455 | 3.738E-07 | 3.706E-07 | 0.881 |
| 3 (free end) | 1.000 | 1.013 | 1.300 | 4.206E-07 | 5.660E-07 | 34.577 |
| Total | - | - | - | 1.422E-06 | 1.561E-06 | 9.75 |

Table 5. Comparison between numerical and analytical results (Model 1)

| Order | Model 1 | | | | | |
|---|---|---|---|---|---|---|
| | Maximum moment (N.m) | | | Strain energy (J) | | |
| | Analytical | Numerical | Error (%) | Analytical | Numerical | Error (%) |
| 0 (trunk) | 192.593 | 204.650 | 6.261 | 1.296E-04 | 1.268E-04 | 2.176 |
| 1 | 56.296 | 59.657 | 5.970 | 4.449E-05 | 4.560E-05 | 2.484 |
| 2 | 14.815 | 15.644 | 5.597 | 1.067E-05 | 1.216E-05 | 14.009 |
| 3 (free end) | 2.963 | 2.999 | 1.230 | 1.231E-06 | 1.213E-06 | 1.476 |
| Total | - | - | - | 1.860E-04 | 1.858E-04 | 0.129 |

The total wall energy obtained by the numerical model and the analytical expression is $1.56\times10^{-8}$ and $5.94\times10^{-6}$ for model 0 and 1, respectively. Therefore, the efficiency of the models 0 and 1 is approximately 100 and 30, respectively. The error of about 34% in the strain energy for the model 0 is due to the stress concentration at extremities together with a poor mesh, which was possible using the student version of the software. The source of the error about 14% in model 1 is yet unknown.

## 5 Conclusions

In this paper, the strain energy stored in 2D elastic trees is evaluated. It is presented a methodology to generate geometries for trees through iterated self-similar systems and the tree extremities withstand moments (model 0) or horizontal forces (model 1). Analytical expressions for the strain energy stored within a tree are deduced as function of the geometric parameters of the tree, and of the external loads. It is noticed that depending on the geometric parameters the energy may be more concentrated within the trunk or at extremities. Two models for intensity of the loads were considered, namely constant independent of the number of branches and equally distributed among the extremities.

The concept of efficiency of a tree in storing energy is defined as the ratio between the energy stored in a tree and the energy stored in a sole trunk both with same volume, where the width of the tree trunk is equal to the width of the sole trunk. Considering a fixed set of parameters $b$, $\lambda$ and $w$ when the external load is independent of the number of branches the efficiency increases exponentially with the number of iterations $n$, both for model 0 and model 1. On the other hand if the load are distributed among the extremities for model 0 the efficiency increases exponentially with $n$ whereas for model 1 the efficiency decreases exponentially with $n$. The reason why this occurs is yet unknown. Considering a fixed $n$ the increase of the ratio sizes $\lambda$ and $w$, in general, induces an increase of the efficiency. However, the parameter $b$ influences the efficiency differently depending on the way the loads are applied. If the loads are constant, independent of the quantity of external branches, the efficiency increases with $b$, exponentially for model 0 and with a limit for model 1. On the other hand, if the load is distributed among the external branches the behavior reverses, i.e. increasing $b$ yields lower efficiencies for both models 0 and 1.

We conclude with the proposed models that the strain energy stored in trees may be very high or very low depending on two aspects: the geometric and evolutionary parameters as well as the way external loads occur, e.g. in the case of wind its drag force. The present model may be used for trees

subject to wind actions in a static way in which the forces are transmitted by the leafs disregarding forces acting on the branches. We visualize two possible applications: artificial trees with leaves associated with photoelectric materials to absorb energy from the sunlight that store minimum strain energy or artificial trees associated with piezoelectric material in order to store high quantities of kinetic energy.

The analytical results for the proposed models were tested through numerical experiments for particular cases. In order to evaluate the particular cases the commercial software ANSYS® Student, which although very limited in terms of degrees of freedom it was enough to indicate the validity of the analytical results.

## Acknowledgements

The authors gratefully acknowledge the financial support provided by the National Council for Scientific and Technological Development (CNPq).

## References

[1] S. P. Beeby, M. J. Tudor and N. M. White. Energy harvesting vibration sources for microsystems applications. *Measurement science and technology*, v. 17, n. 12, p. R175, 2006.
[2] S. Sudevalayam and P. Kulkarni. Energy harvesting sensor nodes: Survey and implications. *IEEE communications Surveys & tutorials*, v. 13, n. 3, p. 443-461, 2010.
[3] D. Castagnetti and E. Radi. A piezoelectric based energy harvester with dynamic magnification: modelling, design and experimental assessment. *Meccanica*, v. 53, n. 11-12, p. 2725-2742, 2018.
[4] D. Castagnetti. Comparison between a wideband fractal-inspired and a traditional multicantilever piezoelectric energy converter. *Journal of Vibration and Acoustics*, v. 137, n. 1, p. 011001, 2015.
[5] D. Castagnetti. Design and characterization of a fractal-inspired multi-frequency piezoelectric energy converter. *Frattura ed Integrità Strutturale*, v. 7, n. 23, p. 87-93, 2013.
[6] B. B. Mandelbrot. An introduction to multifractal distribution functions. In: *Random Fluctuations and Pattern Growth: Experiments and Models.* Springer, Dordrecht, p. 279-291. 1988.
[7] M. Nussenzveig. *Complexidade & Caos*. 2. Ed. Rio de Janeiro: UFRJ/COPEA, 2003.
[8] K. Çelik and E. Kurt. Design and simulation of the antenna for RF energy harvesting systems. In: *2018 6th International Istanbul Smart Grids and Cities Congress and Fair (ICSG)*. IEEE, 2018.
[9] C. Puente et al. Multiband properties of a fractal tree antenna generated by electrochemical deposition. *Electronics Letters*, v. 32, n. 25, p. 2298-2299, 1996.
[10] A. Bakytbekov et al. Fully printed 3D cube-shaped multiband fractal rectenna for ambient RF energy harvesting. *Nano Energy*, v. 53, p. 587-595, 2018.
[11] M. Palandoken and C. Gocen. A modified Hilbert fractal resonator based rectenna design for GSM900 band RF energy harvesting applications. *International Journal of RF and Microwave Computer-Aided Engineering*, v. 29, n. 1, p. e21643, 2019.
[12] M. M. Barros and L. Bevilacqua. Elastic fractal trees: a correspondence among geometry, stress, resilience and material quantity. *Journal of the Brazilian Society of Mechanical Sciences and Engineering*, v. 37, n. 5, p. 1479-1483, 2015.
[13] P. O. Ribeiro. *Estruturas de árvores: Tensão e energia*. 2016. 76 f. TCC (Graduação) - Curso de Engenharia Civil, Universidade Federal de Juiz de Fora, Juiz de Fora, 2016.